Received: 31 January 2024 | Revised: 28 March 2024 | Accepted: 22 April 2024

DOI: 10.1002/nano.202400018

RESEARCH ARTICLE

Nano Select Open Access WILEY

Tetraspanin immunoassay for the detection of extracellular vesicles and renal cell carcinoma

Misba Khan[1,2] | **Md. Khirul Islam**[1,2] | **Mafiur Rahman**[1] | **Bert Dhondt**[3,4] | **Ileana Quintero**[5,6] | **Maija Puhka**[5,6] | **Panu M. Jaakkola**[2,7] | **Urpo Lamminmäki**[1,2] | **Janne Leivo**[1,2]

[1]Department of Life Technologies, Division of Biotechnology, University of Turku, Turku, Finland

[2]InFLAMES Research Flagship Center, University of Turku, Turku, Finland

[3]Department of Urology, Ghent University Hospital, Ghent, Belgium

[4]Cancer Research Institute, Ghent University, Ghent, Belgium

[5]EV and HiPrep Core, Institute for Molecular Medicine Finland FIMM, University of Helsinki, Helsinki, Finland

[6]EV-core facility, University of Helsinki, Helsinki, Finland

[7]Department of Oncology and Radiotherapy and FICAN West Cancer Centre, University of Turku and Turku University Hospital, Turku, Finland

Correspondence
Misba Khan, Department of Life Technologies, Division of Biotechnology, University of Turku, Turku, Finland.
Email: misba.khan@utu.fi

Funding information
European Union's Horizon 2020, Grant/Award Number: Marie Skłodowska-Curie grant agreement No 860303

Abstract

Half of patients with renal cell carcinoma (RCC) develop metastases. New and noninvasive biomarkers are needed for the diagnosis of RCC. The study aims to develop an EV-based assay for the detection of RCC using a highly sensitive nanoparticle-aided time-resolved fluorescence immunoassay (NP-TRFIA). To confirm the presence of tetraspanins on EVs, size exclusion chromatography is used to separate EV- and PE-fractions from RCC4, 786-O, and HEK293 cell lines. EV- and PE-fractions are quantified using NP-TRFIA assays established for CD9, CD63, CD81, and CD151. Tetraspanins are measured from RCC CCM and serum samples of RCC ($n = 14$), benign ($n = 17$), and healthy ($n = 9$) individuals. Among the tetraspanins, CD63 exhibits 3-5-fold higher expression on RCC4 and 786-O CCM compared to HEK293. A sandwich CD63-CD63 assay demonstrates significant discrimination of RCC patients from benign ($p = 0.0003$), and healthy ($p = 0.005$) individuals, respectively. Similarly, the CD81-CD81 assay also enables significant separation of RCC patients compared to benign ($p = 0.014$), and healthy ($p = 0.003$) controls, respectively. This suggests that RCC cell lines and serum of RCC patients show higher amounts of CD63- and CD81-EVs compared to controls. Detection of these EVs using NP-TRFIA approach may play a vital role in the detection of RCC.

KEYWORDS
biomarkers, extracellular vesicles, immunoassay, nanoparticles, renal cell carcinoma, tetraspanins

1 | INTRODUCTION

Renal cell carcinoma (RCC), is among the ten most common cancers in both men and women worldwide.[1] The incidence of RCC varies between genders with men being two-fold more likely to be diagnosed with RCC than women.[2] Among other types of kidney cancers, RCC accounts for 90% of all types and is the third most commonly diagnosed urogenital cancer.[3] At earlier stages, RCC is curable by surgery. The early diagnosis of RCC is difficult as the disease is typically asymptomatic in most patients and is diagnosed incidentally

during abdominal imaging for unrelated issues.[1] However, imaging techniques are not always able to accurately discriminate benign tumors from cancerous ones.[4] Alternatively, kidney biopsy is highly invasive and associated with severe complications such as bleeding, damage to the surrounding structures, pain, infections, etc.[5,6] Reliable noninvasive biomarkers could facilitate the early detection of renal tumors and disease management. Therefore, there is an urgent need for consistent biomarkers that would provide clinically meaningful information directly from patient blood and urine.

Several protein biomarkers have been used for the detection and monitoring of clear cell RCC. The most studied protein biomarkers include carbonic anhydrase 9 (CA9), Von Hippel–Lindau (VHL), and vascular endothelial growth factor (VEGF).[7] CA9 is a transmembrane protein that is overexpressed by cancer cells under hypoxic conditions. This overexpression is thought to be due to the inactivation of the VHL protein which also causes activation of hypoxia-inducible factors (HIFs).[8,9] Activation of HIFs in turn causes overexpression of over 300 genes among them CA9 and VEGF, which is a key factor in angiogenesis. Despite numerous studies reporting elevated levels of CA9 and VEGF in biofluids, none of these biomarkers has yet been established as the gold standard for the detection of RCC.[10] One major challenge with the current biomarkers is the lack of specificity and sensitivity of these biomarkers, which can lead to false positive or false negative results.[11]

Extracellular vesicle (EV) research, with a particular focus on cancer, has experienced a remarkable expansion in the past decade, primarily because EVs offer new possibilities as biomarkers.[12] EVs are nano-sized, lipid-enclosed vesicles typically ranging in size from 40 to 1000 nm.[13,14] EVs are secreted by all cell types under normal as well as diseased conditions and have been reported in all body fluids like blood, urine, sweat, etc.[15–18] EVs contain a cargo of proteins, nucleic acids, and other metabolites and the content of EVs often reflects the cell or tissue of origin, for example, the kidney.[19,20] EVs are considered as a potential source of biomarkers for various diseases including cancers.[21] It has been shown previously that cancer cells release larger amounts of EVs compared to their normal counterparts.[22,23]

Tetraspanins are a superfamily of transmembrane proteins that traverse the lipid bilayer membrane four times. They are found on the plasma membrane surface as well as on the endocytic membranes. Functionally, tetraspanins are involved in cell signaling, adhesion, protein-protein interactions, membrane fusion, and protein trafficking.[24] Several tetraspanins such as CD9, CD63, CD81, and CD151 are found as the most common EV-associated surface markers.[25,26] Indeed, these tetraspanins are the most studied membrane proteins of EVs and they are often used as markers in EV studies.[27] Tetraspanins play a major role in EV formation and have also inspired the development of clinical applications on EV detection.[24] However, tetraspanin profiles are different in different EV sources.[28] The isolation of EVs from biofluids is typically a laborious process complicated by the heterogeneity of EV (subpopulations) and variable purity of EV preparations.[29] Our previous studies have shown that tetraspanins could be detected with simple assays for the quantification of EVs.[30] In a collaborative study, such assays were used to show that there is a higher concentration of CD9 and CD63 positive urinary EVs in men with prostate cancer (PCa) compared to benign prostatic hyperplasia (BPH) when adjusting for prostate specific antigen (PSA) and creatinine values.[31] Yet another study indicated a significant increase in the concentration of CD63-positive urinary EVs in bladder cancer (BlCa) patients compared to normal controls, thus highlighting the potential utility of EV concentration measurement in diagnosing and monitoring of cancers of the urogenital system.[32]

The aim of this study was to establish a simple, but sensitive, nanoparticle-aided time-resolved fluorescence immunoassay (NP-TRFIA) for tetraspanin-associated EVs to explore their potential in noninvasive detection of RCC.

2 | MATERIALS AND METHODS

2.1 | Clinical samples

The study cohort consisted of renal carcinoma patients ($n = 14$), patients with benign prostate hyperplasia or renal conditions ($n = 17$), and healthy individuals ($n = 9$). Patient characteristics are included in Table S1. Healthy control serum samples were voluntarily donated by the lab members of the Biotechnology unit at the University of Turku. Samples were stored at −80°C until further use.

2.2 | Ethical permission

University of Turku ethics committee granted ethical permission for this study. Consent was taken from all the patients before collecting their serum samples. All methods were performed in accordance with relevant guidelines and regulations.

2.3 | Cell culture

Two RCC cell lines, RCC4 overexpressing VHL and 786-0 cells were cultured in Dulbecco's Modified Eagle Medium (DMEM) supplemented with 10% fetal bovine serum (FBS)

and 1% penicillin-streptomycin antibiotics. As a control, the human embryonic kidney cell line HEK293 was cultured in Expi293 medium (Thermo Fischer Scientific, Waltham, MA, USA) following ATCC instructions. Cells were grown in at 37°C and 5% CO_2 in a cell incubator. The cell-culture conditioned medium (CCM) was collected when cell confluency reached 80%–90%. The CCM was centrifuged for 3 minutes at 161 × *g* to remove the cell debris and the supernatant was stored at −80°C until further use.

2.4 | Isolation of EVs

EVs were isolated from the CCM of RCC4-VHL, 786-0, and HEK293 cells. Briefly, 20 mL of CCM was collected for every cell line and centrifuged at 1500 × *g* for 10 minutes to remove further cell debris. The supernatants were subjected to a second spinning for 15 minutes at 3200 × *g* to remove large vesicles and then concentrated using 100 kDa cut-off Vivaspin columns (Sartorius, Germany). The CCM (200 µL) were collected after concentration and used for EV isolation. Izon columns (qEV1/70 nm, code: IC1-70, Immuno Diagnostic Oy) were equilibrated four times with 1X PBS. Using PBS as the running buffer, 16–20 fractions of 200 µL were collected and protein concentration in EV fractions (3-5) and PE fractions (6-9) were checked with NanoDrop (absorbance at 280 nm).

2.5 | EVs-stripped samples

EVs-stripped samples were produced by passing a pool of CCM and serum samples through the ultrafiltration concentrator Vivaspin 2 column (polyethersulfone nanomembrane, MWCO 100 kDa, Sartorius, Germany). This was done by centrifuging the sample in the column at 2000 × *g* for 5–10 minutes. The flow-through was collected and used in the assays. The flow-through should be devoid of EVs as demonstrated previously,[33] due to the fact that EVs generally range in size from 40 to 1000 nm, and the filtration membrane does not permit the passage of particles larger than ca. 10 nm. Prior to usage, the columns were washed with 1X PBS to remove glycerol and other preservatives from the column.

2.6 | Nanoparticle tracking analysis

Nanoparticle tracking analysis (NTA) was performed for the cell line-derived EVs using the previously described protocol.[34] The particle number and size distribution of the EV samples were analyzed using an NTA instrument (Particle Metrix Zetaview PMX-120, Ammersee, Germany) which was equipped with a blue laser (488 nm, 70 mW) and sCMOS camera (Hamamatsu Photonics K.K., Hamamatsu, Japan). To record the videos, the camera level was set to 14, the screen gain was set to 1.0, and the temperature was maintained at 22.02°C. EV samples were measured three times with a video length of 90 seconds. The data obtained was analyzed with Nanosight software v3.0, using threshold 5 and gain 10.

2.7 | Transmission electron microscopy (TEM)

EVs were prepared for TEM following a protocol previously described by Puhka et al.[34] Briefly, to concentrate the EVs, samples were centrifuged with Amicon Ultra 0.5 mL Centrifugal Filters with a 10 kDa cutoff for 15 minutes. Then, EVs were loaded to carbon coated and glow discharged 200 mesh copper grids with pioloform support membrane. EVs were fixed with 2% paraformaldehyde (PFA) in $NaPO_4$ buffer pH7, washed and then stained with 2% neutral uranyl acetate. EVs were further stained and embedded in a mixture of uranyl acetate and methyl cellulose (1.8/0.4%). The EVs were viewed using TEM in a Jeol JEM-1400 microscope (Jeol Ltd., Tokyo, Japan) operating at 80 kV. Images were taken with a Gatan Orius SC 1000B CCD camera (Gatan Inc., USA) with a resolution of 4008 × 2672 px image size and no binning.

2.8 | Labeling of capture antibodies with biotin

Monoclonal antibodies (mAbs) anti-CD63 (clone 556019) (catalog # 556019), and -CD81 (clone 555675) (catalog # 555675) were purchased from BD Biosciences (Vantaa, Finland) and anti-CD9 (clone 209306) (catalog # MAB1880) and -CD151 (clone 210127) (catalog # Mab 1884) were purchased from R&D systems (Abingdon, UK). The antibodies used in this study are human specific monoclonal antibodies. The antibodies were labeled with biotin according to the previously described protocol.[35] In brief, biotin isothiocyanate (BITC) was dissolved in ethanol to a final concentration of 10 mM. The antibody solution was adjusted to a pH of 9.8 using 0.5 M carbonate buffer. Then, a 40-fold excess of biotin was added to the antibody solution. The final protein concentration was 2 mg/mL. The reaction mixture was incubated at room temperature (RT) for 4 hours. After incubation, the biotinylated antibodies were purified by removing the unreacted BITC by gel filtration with NAP-5 or NAP-10 columns (GE-Illustra, Diegem, Belgium). TSA buffer (pH 7.5, 50 mmol/L Tris-HCL, 150 mmol/L NaCl, and 0.5 g/L NaN_3) was used in gel filtration. The biotinylated antibodies were stabilized with

1 g/L BSA (Bioreba, Nyon, Switzerland) and were stored at +4°C.

2.9 | Labeling of detection antibodies with europium

The detection mAbs CD9, CD63, CD81, and CD151 were coated on europium nanoparticles (Eu^{3+}-NPs), according to a previously described method with some minor modifications.[36] The amino groups of antibodies were covalently coupled to the activated carboxyl groups present on the Eu^{3+}-NPs. The concentration of antibodies used was 0.1 mg/mL and 1×10^{12} Eu^{3+}-NPs were used per reaction. The particles were washed with conjugation buffer (50 mM MES, pH 6.1) using Nanosep 300 kDa Omega centrifugal filters (Pall Corp., Ann Arbor, MI, USA). The nanoparticles were activated with 8 mmol/L N-hydroxysulfosuccinimide (NHS) and 2.6 mmol/L N-(3-dimethylaminopropyl)-N-ethylcarbodiimide (EDC) (Sigma–Aldrich, St. Louis, Mo, USA). The reaction mixture was then prepared in which the activated particles were coupled with antibodies in MES buffer (50 mM, pH 6.1, 100 mM NaCl). Next, 1% bovine serum albumin (BSA) was added to the reaction mixture to block the remaining active sites on the particles. This was followed by an incubation for 30 minutes at RT. The reaction mixture was stored overnight on a rotary mixer at +4°C. The next morning, the mixture was concentrated using a Nanosep centrifugal filter device (300 kDa) at 5300 × *g* and washed in storage buffer (25 mM Tris, 150 mM NaCl, 0.1% NaN_3 pH 8). The conjugated NPs were stored in the storage buffer supplemented with a final concentration of 0.2% BSA and were finally stored at +4°C until further use.

2.10 | Immunoassay

Two types of time-resolved immunofluorescence-based assays set up as shown in Figure 1. We started by using a direct assay which is based on the passive coating of the sample EVs. In this assay, 10 µL of the sample diluted in PBS (30 µL/well) were immobilized in a 96-well Maxisorp plate (KaiSA96, Kaivogen, Turku, Finland). The plates were incubated for 2 hours at +35°C, followed by washing the wells 2 times with wash buffer (product #:42-01TY, Kaivogen, Turku, Finland) in a DELFIA plate washer. Then, 2% BSA in TSA buffer, in a volume of 30 µL/well along with red assay buffer (product #:42-02TY, Kaivogen, Turku, Finland) in a volume of 20 µL/well was added. The plates were covered with the tape and incubated for 2 hours at +4°C followed by two washes. In a final volume of 30 µL, 1×10^7 of NPs were added to each well and incubated for 1 hour at RT on a plate shaker with slow shaking.

Next, sandwich immunoassays were employed for the characterization of clinical serum samples. This is due to their heightened sensitivity, in comparison to direct assays. The utilization of two antibodies to detect the antigen confers increased specificity to sandwich assays.[37] An additional key advantage of the sandwich assay is its capability to identify and analyze distinct subsets of EVs based on the specificity of the capture antibody utilized.

For the sandwich assay, the biotinylated capture antibody (100 ng/well), diluted in the red assay buffer, was let to immobilize on the streptavidin-coated wells (KaiSA96, Kaivogen, Turku, Finland) in a volume of 30 µL/well. After 1 hour incubation at RT, plates were washed two times with the wash buffer. Then, the samples were diluted in the red assay buffer and added in a final volume of 50 µL/well. This was followed by 1 hour incubation with slow shaking at RT. After two washings, tracers (antitetraspanin antibodies coated on Eu^{3+}-NPs) 2×10^7 NPs were added in a final volume of 30 µL/well. After 1.5 hours incubation at RT, the plates were washed four times. Then, the signal was measured (λex: 340 nm; λem: 615 nm) with a Victor 1420 multilabel counter (PerkinElmer) using the program europium from the surface. All measurements were conducted in triplicates and signal/background was picked up for analysis.

2.11 | Statistics and data analysis

Statistical analysis was performed using IBM SPSS Statistics (version 28) and Origin (version 2016) for Windows. A nonparametric Kruskal–Wallis test was used to calculate statistical significance and a *p*-value below 0.05 was considered significant. For the box plots and heatmap we used R software (http://www.r-project.org/), version 3.6.2 and Tidyverse (version 1.3.0),[38] and ggpubr (version 0.2.5) R packages.[39] The receiver operating characteristic (ROC) curve was made with SPSS software. The area under the curve (AUC) was measured specificity versus sensitivity of the assay.

3 | RESULTS

3.1 | EVs characterization and analysis

EV- and PE-fractions from size-exclusion chromatography were assessed for tetraspanin (CD9, CD63, CD81, and CD151) marker levels with a direct assay. As shown in Figure 2A, EV-fractions, derived from RCC4 cell line, produced higher signals than the PE-fractions in the case of all four tetraspanins, fold difference ranging from 2 to 11. Next, sandwich assays were performed using monoclonal CD63 and CD81 antibody as captures as well as the tracers, that is,

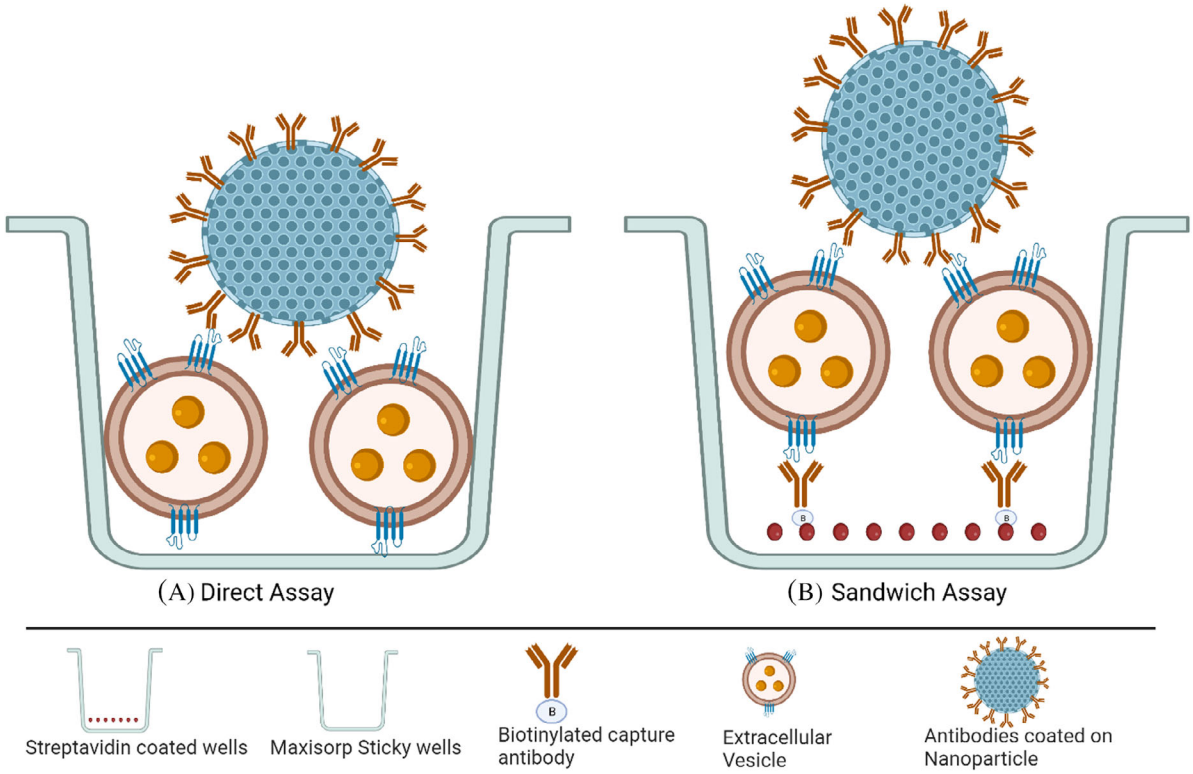

FIGURE 1 Schematic representation of the immunoassays. A, In a direct assay, extracellular vesicles (EVs) were passively immobilized on Maxisorp plate and subsequently detected with the antitetraspanin antibody coated on nanoparticles. B, In a sandwich assay, biotinylated antibodies were immobilized on the surface of the streptavidin-coated microtiter wells for capturing the EVs. The captured EVs were then detected with the antitetraspanin antibody coated on nanoparticles.

CD63-CD63 and CD81-CD81 assays and their efficacy was assessed using RCC4 CCM and RCC pooled serum. Significant signals were observed from the assays when RCC4 CCM and serum of RCC samples were used (Figure 2B). The assay interference was evaluated from (negative) control samples, that is, EV stripped CCM and serum as well as DMEM medium with 10% FBS. The signals obtained from these samples did not show any significant signal intensity (Figure 2B). The total number of EVs and their size were measured by NTA (Figure 2C). The NTA data showed a range of 3.7×10^7 to 5.2×10^7 particles/mL in isolated-EVs from HEK293, RCC4, and 786-O cells and sizes mainly below 500 nm. Moreover, the integrity and morphology of the cell-derived EVs were assessed using TEM that revealed typical vesicles surrounded by a lipid bilayer with approximate diameters of up to 500 nm (Figure 2D). As a negative control, the corresponding PE fractions from size-exclusion chromatography showed generally a lack of EVs by TEM (Figure S1).

3.2 | Characterization of cell line-derived material in a sandwich assay

To analyze the performance of the tetraspanins in the cell line-derived material, we set up a series of sandwich assays in which various combinations of antitetraspanin antibodies were used for capturing and tracing the EVs. Among the different assay configurations, the CD63-CD63 assay showed higher expression on CCM-derived from RCC4 and 786-O cell lines compared to HEK293 control. CD63-CD63 assay showed a 4-6-fold higher expression on RCC4 and 786-O cell lines compared to HEK293 control (Figure 3). Among the other tetraspanin assay combinations, CD63-CD151 and CD81-CD9 assays showed differential expression and were also chosen for further analysis.

From the conducted assays, CD63 emerged as a promising candidate, exhibiting a notably elevated expression level in RCC CCM compared to the control derived from HEK 293 cells.

3.3 | Characterization of clinical serum samples

We proceeded with the assays configurations that showed statistically significant differences with cell line materials and tested their performance with clinical serum samples from healthy ($n = 9$), benign ($n = 17$), and RCC ($n = 14$) patients. The CD63-CD63 assay demonstrated

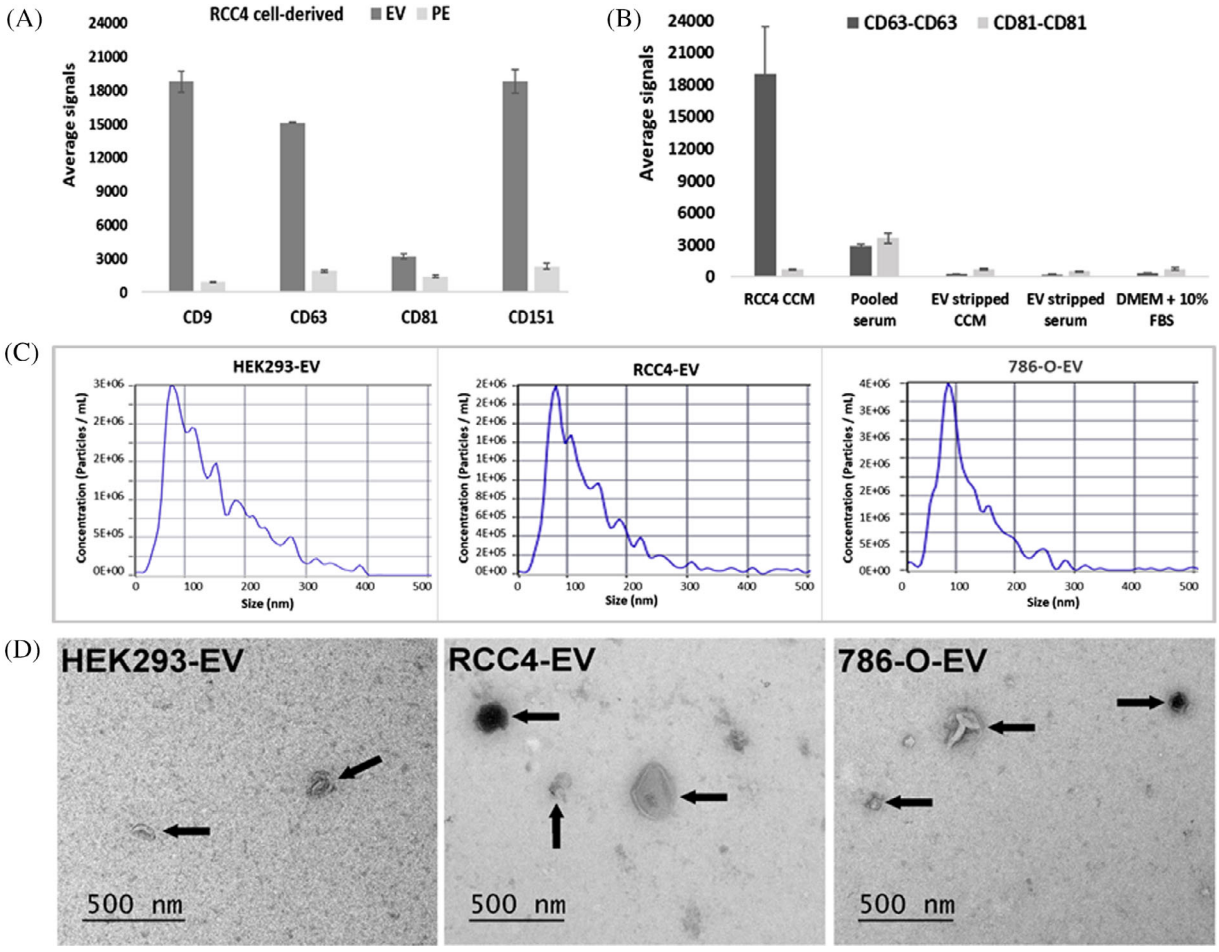

FIGURE 2 The extracellular vesicles (EVs) characterization and quality control. In direct assay, (A) EVs quality was assessed by comparing EV-and PE-fractions (F1-F12) of RCC4 cell line for the levels of CD9, CD63, CD81, and CD151 markers. In sandwich assay, (B) the assay specificity and interference were checked using RCC4 CCM and serum of RCC samples as well as in the presence of EV stripped CCM and serum, and 10% FBS added DMEM medium. EVs were characterized by (C) nanoparticle tracking analysis (NTA) for total number of particles, and (D) TEM for the structure and integrity of vesicles derived from control HEK293 and renal cancer RCC4 and 786-O cell lines. (Here, S/B, signal to background, TRF, time-resolved fluorescence). All analysis was conducted in triplicates.

significant discrimination of RCC patients from benign (3-fold; $p = 0.0003$), and healthy (4-fold; $p = 0.005$) individuals, respectively. Similarly, the CD81-CD81 assay also enabled significant separation of RCC patients compared to benign (2-fold; $p = 0.014$), and healthy (3-fold; $p = 0.003$) controls, respectively (Figure 4A). In addition, we also performed CD63-CD151, CD81-CD9, and CA9-CA9 assays using the clinical serum samples. The CD63-CD151 assay showed limited separation among the three groups, and no discrimination was observed with CD81-CD9 and CA9-CA9 assays (Figure S2).

Our findings demonstrated that the CD63-CD63 and CD81-CD81 assay configurations effectively discriminated RCC patients from both benign and healthy individuals.

The performance of the CD63-CD63 and CD81-CD81 assays was analyzed by plotting the Receiver Operating Characteristic (ROC curve) (Figure 4B). The samples were divided into two groups, that is, noncancer and cancer group. Noncancer group consisted of 26 samples (healthy = 9 and benign = 17) and cancer group consisted of 14 samples. The calculated AUC was 0.849 and 0.799 for CD63-CD63 and CD81-CD81 assays, respectively.

4 | DISCUSSION

In this study, we describe a straightforward tetraspanin-enriched EVs targeting immunoassay approach with promising insights into the noninvasive detection of RCC. The assay relies on the highly sensitive nanoparticle-aided time-resolved fluorescence immunoassay concept and allows the analysis of unprocessed serum samples. We demonstrated the presence of specific tetraspanins in the

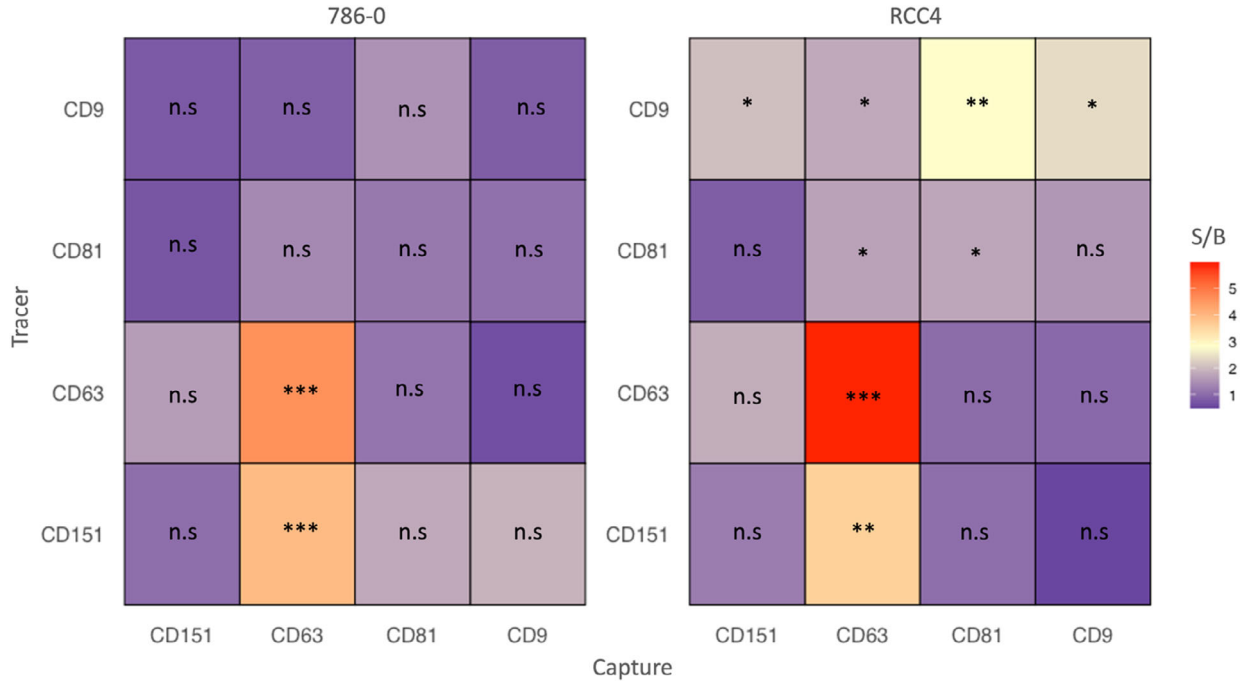

FIGURE 3 Testing tetraspanin-binding assay configurations with CCM-derived from renal cancer RCC4 and 786-O cells. The heatmap of the tetraspanin expression for CD9, CD63, CD81, and CD151. Each of the tetraspanin antibody was tested both as a capture (x) and a tracer (y) in a sandwich immunoassay and the heatmap depicts the fold-change (S/B) between 789-0/RCC4 and HEK293. (*$p < 0.05$, **$p < 0.01$, ***$p < 0.001$).

EV preparations isolated by size-exclusion chromatography from RCC cell culture medium using the NP-TRFIA. This study also validated the high abundance of specific tetraspanins such as CD63 and CD81 in the clinical serum samples from RCC patients compared to the samples from healthy individuals or individuals with benign renal conditions.

The NP-TRFIA approach employs antibody coated nanoparticles, harboring up to 30000 fluorescent lanthanide chelates for quick (<4 hours), simple, highly sensitive and scalable detection of EVs. The NP concept not only amplifies the detectable signal but also augments the assay's sensitivity through the avidity effect from multivalent binding.[40] Previously we have reported that our nanoparticle-aided-TRFIA assay requires only 4–13 ng (0.04–0.06 ng/mL) of protein from isolated EVs for detection,[30] making it considerably more sensitive than the reported tetraspanin targeting ELISA assay for EVs.[25] Compared to flow-cytometry based detection of EVs, it also has the advantage of use of significantly less complex instrumentation.[28,41] Previously we have shown that tetraspanin-positive EVs are elevated in urine from prostate cancer patients as well as serum of breast and colorectal cancer patients.[31,42,43] In different studies, tetraspanins have been used for measuring the bulk of EVs by flow cytometry[28,41] and ELISA assay.[25]

We applied NP-TRFIA concept to assess the relevance of several tetraspanins CD9, CD63, CD81, and CD151 in the context of RCC by using a step-by-step approach to move from less demanding samples (pure cell line derived EVs) to more complex matrixes, that is, cell culture media and clinical serum samples. In our study, direct assays were employed for the analysis of isolated EVs, while sandwich assays, recognized for their versatility, were utilized for both purified EVs, CCM as well as clinical serum samples. The sandwich assays were selected based on their flexibility in detecting various sample types, including those with complex matrices, without necessitating prior isolation of EVs. In addition, our assays exhibit exceptional sensitivity and can be carried out using a minimal sample volume of 5–10 μL. Herein, we analyzed the performance of different capture-tracer pairs in the detection of teraspanins CD9, CD63, CD81, and CD151. Tetraspanin expression on EVs was explored by measuring the expression levels of tetraspanin markers (CD9, CD63, CD81, and CD151). In the cell line-based studies CD63 clearly stood out with a significantly more prominent expression in the EVs of RCC cell lines compared to those of the control cell line HEK293 (Figure 2A). We extended the findings to RCC cell line-derived CCM and observed that the assay utilizing CD63 as both the capture and the tracer exhibited higher expression in CCM compared to control sources. This

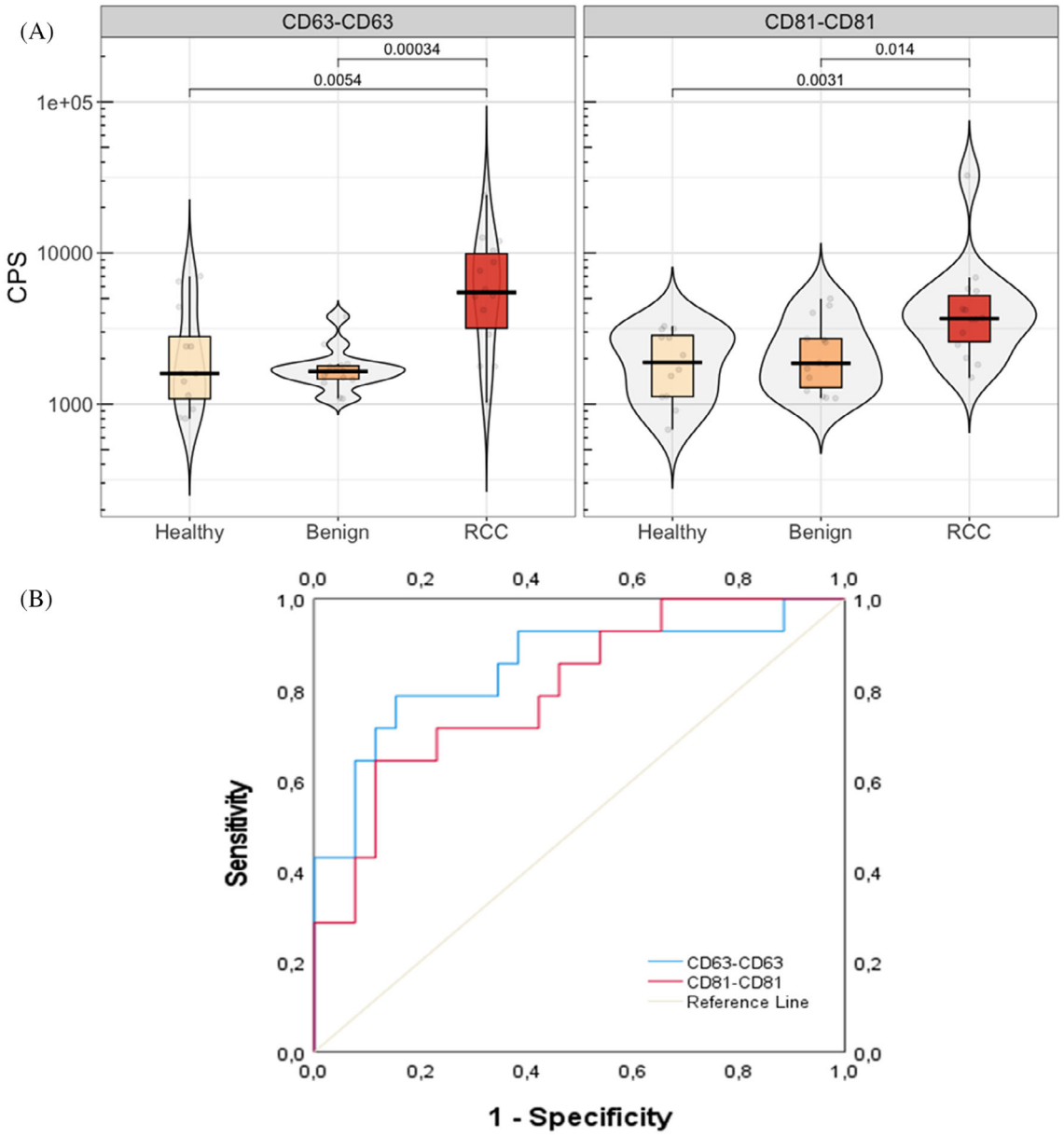

FIGURE 4 Characterization of clinical serum samples. A, The performance of CD63-CD63 and CD81-CD81 assay in healthy ($n = 9$), benign ($n = 17$) and RCC ($n = 14$) patients. The p-values were calculated using Mann–Whitney U Test. B, The receiver operating characteristic (ROC) curve displaying the area under the curve (AUC) of CD63-CD63 (blue) and CD81-CD81 (red) assay from noncancer ($n = 26$) and RCC ($n = 14$) patients.

finding on the prominent role of CD63 correlates with the observations of a previous study by Duijvesz et al., where the monoclonal tetraspanin-specific antibodies (CD9 and CD63) were employed for capturing and detecting EVs from the urine of prostate cancer patients.[31] We further selected assay configurations based on their significant differences observed with cell line materials and evaluated their performance using clinical serum samples from healthy individuals, benign cases, and RCC patients. Similar outcome was then also obtained using a small panel of individual clinical serum samples. RCC patient samples showed higher expression of CD63 compared to benign (3-fold; $p = 0.0003$), and healthy (4-fold; $p = 0.005$) controls. Likewise, CD81 expression was also higher in RCC patient samples compared to benign (2-fold; $p = 0.014$), and healthy (3-fold; $p = 0.003$) controls (Figure 4).

In addition to CD63-CD63 assay, CD63-CD151 and CD81-CD9 assays showed significantly higher S/B ratios with RCC-CCM compared to controls (Figure 3). Then, tested with the same cohort of clinical samples, only CD63-CD151 was able to separate the three groups (Figure S2). In a

recent study, Himbert et al. suggested that Carbonic anhydrase 9 (CA9) is a new promising protein biomarker on EVs derived from RCC patients' tissue samples.[44] Thereby, we also tested CA9-CA9 assay where anti-CA9 antibodies were used as a capture and tracer. Although the CA9-CA9 assay was able to separate healthy individuals from the RCC patients ($n = 0.009$), this assay was not able to separate benign cases from RCC patients (Figure S2). This suggests that the CA9 assay may not be specific enough for the RCC when applied to serum samples.

To analyze the effects of possible interference of FBS contained bovine EVs or other sample components in our assays, we performed the total CD63 and total CD81 assays with DMEM supplemented with 10% FBS, EV-stripped CCM and RCC serum samples. We found no expression of CD63 and CD81 on the material derived from FBS and EV-stripped matrix of CCM and serum samples. The significant signals were derived only from EVs in the sample (Figure 2B).

CD63 and CD81 are both involved in cell adhesion, signaling, and membrane organization.[45] In the context of RCC, their elevated expression might indicate their participation in processes that are unique to or heightened in cancer cells. This could include interactions with other molecules, signaling pathways, or cellular functions that contribute to the aggressive behavior of cancer cells. Likewise, EVs are released by cancer cells during hypoxia within the solid tumors and this facilitates communication with the surrounding tissues.[46] These EVs play pivotal roles in shaping the tumor microenvironment and are associated with crucial processes like angiogenesis, invasion, metastasis, drug resistance, and immune evasion.[47] The cancer cells undergo further adaptations in response to hypoxia that include alterations in metabolism, pH regulation, and strategies to evade the immune system which collectively promotes the tumor growth, survival, and resistance to therapy.[48] In summary, processes like hypoxia, tumor growth, angiogenesis, and immune evasion are responsible for the secretion of EVs from cancer cells, thus highlighting the role of cancer derived EVs in cancer progression and resistance to therapeutic interventions.

In summary, the study demonstrated that the expression of CD63 and CD81 tetraspanins were significantly elevated in RCC patient samples compared to both benign conditions and healthy controls. This suggests that these proteins might play a role in the development or progression of RCC and could potentially serve as biomarkers for diagnosis or monitoring of the disease. As the EV tetraspanin assays have been shown to detect several types of cancers,[31,42,43] they hold promise for a broad-spectrum screening tool for pan-cancer detection and further developed into a cancer-type specific multimarker panel by incorporating different tetraspanins and other markers.

5 | CONCLUSION

In conclusion, our study highlights the potential of utilizing EVs enriched with tetraspanins, particularly CD63 and CD81, as promising biomarkers for the noninvasive detection of RCC. Through the implementation of a highly sensitive nanoparticle-aided time-resolved fluorescence immunoassay, we observed significantly higher levels of CD63- and CD81-enriched EVs in both RCC cell lines and serum samples from RCC patients compared to benign and healthy controls. Our findings underscore the significance of EV-based assays as a means of diagnosing RCC. By harnessing the diagnostic potential of EVs, we aim to address the current need for new and noninvasive biomarkers in RCC diagnosis. The significant discrimination achieved between RCC patients and control groups, as demonstrated by the CD63-CD63 and CD81-CD81 assays, emphasizes the clinical relevance of our approach. However, the small sample size used in this study is a significant limitation, and further research with larger cohorts is required to validate the assay's efficacy. Continued research in this area holds promise for the development of effective diagnostic tools that can improve the early detection of RCC, ultimately contributing to better patient outcomes.

ACKNOWLEDGMENTS

The research work was made possible thanks to the support of the ProEVLifeCycle project, which received funding from the European Union's Horizon 2020 research and innovation program. This research was supported by the Research Council of Finland's Flagship InFLAMES (337530 and 357910). We would like to express our gratitude to Turku Prostate Cancer Consortium (TPCC) for generously providing the clinical samples that were crucial to the success of this study. Additionally, we would like to extend our thanks to all the patients for their samples. We also acknowledge the support of the DPT-University of Turku graduate school, which provided invaluable assistance throughout the study.

CONFLICT OF INTEREST STATEMENT

The authors declare no conflicts of interest.

DATA AVAILABILITY STATEMENT

The data supporting the findings of this study are openly available online without any restrictions. Researchers are encouraged to access and utilize the data for further analysis and research purposes.

ORCID

Misba Khan https://orcid.org/0000-0002-3726-4654

REFERENCES

1. R. E. Gray, G. T. Harris, *Am. Fam. Physician* **2019**, *99*, 179.
2. K. Hemminki, A. Försti, A. Hemminki, B. Ljungberg, O. Hemminki, *PLoS One* **2021**, *16*, e0253236.
3. N. Petejova, A. Martinek, *Biomed. Pap. Med. Fac. Univ. Palacky Olomouc. Czech Repub.* **2016**, *160*, 183.
4. T. Shin, V. A. Duddalwar, O. Ukimura, T. Matsugasumi, F. Chen, N. Ahmadi, A. L. de Castro Abreu, H. Mimata, I. S. Gill, *Urol. Int.* **2017**, *99*, 229.
5. E. D. Poggio, R. L. McClelland, K. N. Blank, S. Hansen, S. Bansal, A. S. Bomback, P. A. Canetta, P. Khairallah, K. Kiryluk, S. H. Lecker, G. M. McMahon, P. M. Palevsky, S. Parikh, S. E. Rosas, K. Tuttle, M. A. Vazquez, A. Vijayan, B. H. Rovin, *Clin. J. Am. Soc. Nephrol.* **2020**, *15*, 1595.
6. G. Singh, L. Singh, R. Ghosh, D. Nath, A. K. Dinda, *World J. Nephrol.* **2016**, *5*, 461.
7. A. Mickley, O. Kovaleva, J. Kzhyshkowska, A. Gratchev, *EPMA J.* **2015**, *6*, 20.
8. J. Courcier, A. De La Taille, M. Nourieh, I. Leguerney, N. Lassau, A. Ingels, *Int. J. Mol. Sci.* **2020**, *21*, 7146.
9. B. B. McGuire, J. M. Fitzpatrick, *Curr. Opin. Urol.* **2009**, *19*, 441.
10. J. Kapoor, Claps, F., Mir, C., Ischia, J., *Société Internationale d'Urologie Journal* **2021**, *2*, 43.
11. O. Bratu, D. Mischianu, D. Marcu, D. Spinu, L. Iorga, A. Cherciu, I. Balescu, N. Bacalbasa, C. Diaconu, C. Savu, R. Anghel, *Exp. Ther. Med.* **2021**, *22*, 1297.
12. C. Williams, F. Royo, O. Aizpurua-Olaizola, R. Pazos, G. J. Boons, N. C. Reichardt, J. M. Falcon-Perez, *J. Extracell. Vesicles* **2018**, *7*, 1442985.
13. M. Martins Á, C. C. Ramos, D. Freitas, C. A. Reis, *Cells* **2021**, *10*, 109.
14. L. Yuka, K. Eisuke, Y. Tomoyoshi, I. Yasushi, I. Koshi, *Anal. Chem.* **2023**, *95*, 14159.
15. J. Macedo-da-Silva, V. F. Santiago, L. Rosa-Fernandes, C. R. F. Marinho, G. Palmisano, *Mol. Immunol.* **2021**, *135*, 226.
16. S. Keller, A. K. König, F. Marmé, S. Runz, S. Wolterink, D. Koensgen, A. Mustea, J. Sehouli, P. Altevogt, *Cancer Lett.* **2009**, *278*, 73.
17. S. Alvarez, C. Suazo, A. Boltansky, M. Ursu, D. Carvajal, G. Innocenti, A. Vukusich, M. Hurtado, S. Villanueva, J. E. Carreño, A. Rogelio, C. E. Irarrazabal, *Transplant Proc.* **2013**, *45*, 3719.
18. C. X. Wu, Z. F. Liu, *J. Invest. Dermatol.* **2018**, *138*, 89.
19. M. Ludwig, R. Rajvansh, J. M. Drake, *Endocrinology* **2021**, *162*, 139.
20. O. P. Dwivedi, K. Barreiro, A. Käräjämäki, E. Valo, A. K. Giri, R. B. Prasad, R. D. Roy, L. M. Thorn, A. Rannikko, H. Holthöfer, K. M. Gooding, S. Sourbron, D. Delic, M. F. Gomez, P. H. Groop, T. Tuomi, C. Forsblom, L. Groop, M. Puhka, *iScience* **2023**, *26*, 106686.
21. R. C. Zieren, L. Dong, P. M. Pierorazio, K. J. Pienta, T. M. de Reijke, S. R. Amend, *Med. Oncol.* **2020**, *37*, 28.
22. B. Pang, Y. Zhu, J. Ni, J. Thompson, D. Malouf, J. Bucci, P. Graham, Y. Li, *Theranostics* **2020**, *10*, 2309.
23. N. Karimi, R. Dalirfardouei, T. Dias, J. Lötvall, C. Lässer, *J. Extracell. Vesicles* **2022**, *11*, e12213.
24. Z. Andreu, M. Yáñez-Mó, *Front. Immunol.* **2014**, *5*, 442.
25. M. Logozzi, A. De Milito, L. Lugini, M. Borghi, L. Calabrò, M. Spada, M. Perdicchio, M. L. Marino, C. Federici, E. Iessi, D. Brambilla, G. Venturi, F. Lozupone, M. Santinami, V. Huber, M. Maio, L. Rivoltini, S. Fais, *PLoS One* **2009**, *4*, e5219.
26. R. R. Mizenko, T. Brostoff, T. Rojalin, H. J. Koster, H. S. Swindell, G. S. Leiserowitz, A. Wang, R. P. Carney, *J. Nanobiotechnology* **2021**, *19*, 250.
27. J. Jankovičová, P. Sečová, K. Michalková, J. Antalíková, *Int. J. Mol. Sci.* **2020**, *21*, 7568.
28. C. Campos-Silva, H. Suárez, R. Jara-Acevedo, E. Linares-Espinós, L. Martinez-Piñeiro, M. Yáñez-Mó, M. Valés-Gómez, *Sci. Rep.* **2019**, *9*, 2042.
29. E. Willms, C. Cabañas, I. Mäger, M. J. A. Wood, P. Vader, *Front. Immunol.* **2018**, *9*, 738.
30. M. K. Islam, P. Syed, L. Lehtinen, J. Leivo, K. Gidwani, S. Wittfooth, K. Pettersson, U. Lamminmäki, *Sci. Rep.* **2019**, *9*, 10038.
31. D. Duijvesz, C. Y. Versluis, C. A. van der Fels, M. S. Vredenbregt-van den Berg, J. Leivo, M. T. Peltola, C. H. Bangma, K. S. Pettersson, G. Jenster, *Int. J. Cancer* **2015**, *137*, 2869.
32. L. G. Liang, M. Q. Kong, S. Zhou, Y. F. Sheng, P. Wang, T. Yu, F. Inci, W. P. Kuo, L. J. Li, U. Demirci, S. Wang, *Sci. Rep.* **2017**, *7*, 46224.
33. R. Kornilov, M. Puhka, B. Mannerström, H. Hiidenmaa, H. Peltoniemi, P. Siljander, R. Seppänen-Kaijansinkko, S. Kaur, *J. Extracell. Vesicles* **2018**, *7*, 1422674.
34. M. Puhka, M. E. Nordberg, S. Valkonen, A. Rannikko, O. Kallioniemi, P. Siljander, T. M. Af Hällström, *Eur. J. Pharm. Sci.* **2017**, *98*, 30.
35. M. K. Islam, P. Syed, B. Dhondt, K. Gidwani, K. Pettersson, U. Lamminmäki, J. Leivo, *Anal. Biochem.* **2021**, *628*, 114283.
36. J. Terävä, L. Tiainen, U. Lamminmäki, P. L. Kellokumpu-Lehtinen, K. Pettersson, K. Gidwani, *PLoS One* **2019**, *14*, e0219480.
37. S. Sakamoto, W. Putalun, S. Vimolmangkang, W. Phoolcharoen, Y. Shoyama, H. Tanaka, S. Morimoto, *J. Nat. Med.*. **2018**, *72*, 32.
38. H. Wickham, M. Averick, J. Bryan, W. Chang, L. D. A. McGowan, R. François, G. Grolemund, L. Henry, A. Hayes, J. Hester, M. Kuhn, T. L. Pedersen, E. Miller, S.M. Bache, K. Müller, J. Ooms, D. P. Seidel, V. Spinu, K. Takahashi, D. Vaughan, C. Wilke, K. Woo, H. Yutani, *JOSS*, **2019**, *4*, 1686.
39. A. Kassambara, ggpubr: 'ggplot2' Based Publication Ready Plots, **2023**, 0.6.0.
40. H. Kekki, M. Peltola, S. van Vliet, C. Bangma, Y. van Kooyk, K. Pettersson, *Clin. Biochem.* **2017**, *50*, 54.
41. H. Suárez, A. Gámez-Valero, R. Reyes, S. López-Martín, M. J. Rodríguez, J. L. Carrascosa, C. Cabañas, F. E. Borràs, M. Yáñez-Mó, *Sci. Rep.* **2017**, *7*, 11271.
42. J. Terävä, A. Verhassel, O. Botti, M. K. Islam, J. Leivo, S. Wittfooth, P. Härkönen, K. Pettersson, K. Gidwani, *Cancer Rep. (Hoboken)* **2022**, *5*, e1540.
43. R. Vinod, R. Mahran, E. Routila, J. Leivo, K. Pettersson, K. Gidwani, *Int. J. Mol. Sci.* **2021**, *22*, 10329.
44. D. Himbert, P. Zeuschner, H. Ayoubian, J. Heinzelmann, M. Stöckle, K. Junker, *Diagnostics (Basel)* **2020**, *10*, 1034.
45. C. M. Termini, J. M. Gillette, *Front. Cell. Dev. Biol.* **2017**, *5*, 34.
46. K. K. W. To, W. C. S. Cho, *Cancer Drug Resist.* **2022**, *5*, 577.
47. P. C. McDonald, S. C. Chafe, S. Dedhar, *Front. Cell. Dev. Biol.* **2016**, *4*, 27.

48. R. Jafari, R. Rahbarghazi, M. Ahmadi, M. Hassanpour, J. Rezaie, *J. Transl. Med.* **2020**, *18*, 474.

SUPPORTING INFORMATION

Additional supporting information can be found online in the Supporting Information section at the end of this article.

How to cite this article: M. Khan, M. K. Islam, M. Rahman, B. Dhondt, I. Quintero, M. Puhka, P. M. Jaakkola, U. Lamminmäki, J. Leivo, *Nano Select* **2024**, e2400018.
https://doi.org/10.1002/nano.202400018